IEEE Access
Multidisciplinary ⋮ Rapid Review ⋮ Open Access Journal

Received May 23, 2018, accepted June 23, 2018, date of publication July 3, 2018, date of current version July 19, 2018.

Digital Object Identifier 10.1109/ACCESS.2018.2851940

A Wireless Implantable Sensor Design With Subcutaneous Energy Harvesting for Long-Term IoT Healthcare Applications

TAIYANG WU, (Student Member, IEEE), JEAN-MICHEL REDOUTÉ, (Senior Member, IEEE), AND MEHMET RASIT YUCE, (Senior Member, IEEE)

Department of Electrical and Computer Systems Engineering, Monash University, Melbourne, VIC 3800, Australia

Corresponding author: Mehmet Rasit Yuce (mehmet.yuce@monash.edu)

This work was supported by the Australian Research Council Future Fellowships under Grant FT130100430.

ABSTRACT In this paper, a wireless implantable sensor prototype with subcutaneous solar energy harvesting is proposed. To evaluate the performance of a flexible solar panel under skin, ex-vivo experiments are conducted under natural sunlight and artificial light sources. The results show that the solar panel covered by a 3 mm thick porcine flap can output tens of microWatts to a few milliWatts depending on the light conditions. The subcutaneous solar energy harvester is tested on different body parts, which suggests the optimal position for the harvester to implant is between neck and shoulder. A wireless implantable system powered by the subcutaneous energy harvester is presented, which consists of a power management circuit, a temperature sensor, and a Bluetooth low energy module. An application is developed for data visualization on mobile devices, which can be a gateway for future IoT-based healthcare applications. The entire device is embedded in a transparent silicone housing (38 mm $\times$ 32 mm $\times$ 4 mm), including a 7 mAh rechargeable battery for energy storage. The average power consumption of the implants is about 30 μW in a 10 min operation cycle. With the subcutaneous solar energy harvester, the self-powered operation of the implantable sensor prototype is demonstrated by long-term experimental results. Two worst-case scenarios (no exposure to light and battery depletion) are considered with ex-vivo experiment simulations.

INDEX TERMS Implantable biomedical device, energy harvesting, wireless communication, self-powered system, long-term healthcare.

I. INTRODUCTION

With the increase of average human lifespan, chronic diseases are one of the predominant challenges to people's health globally [1]. Many chronic diseases, such as cardiovascular, neurological, and glucose disorders, can be treated or monitored by implanted biomedical devices [2]–[5]. One of the limitations in the development of implantable electronic devices is the power supply, as most of the implants use batteries with finite lifetime [6]. Periodical surgeries for battery replacement will increase patients' physical, psychological, and financial burdens. With the emerging of Internet of Things (IoT) in healthcare monitoring, a continuous power source is necessary to maintain long-term connectivity [7]. Energy harvesting technique is a promising solution to the powering issue of implantable electronics.

Researchers worldwide have proposed several implantable energy harvesting methods using different sources, such as thermal energy, mechanical motion, and radio frequency (RF) energy transfer [6], [8], [9]. In [10], Kim *et al.* propose a flexible piezoelectric energy harvester, which generates electricity from the contraction and relaxation of a porcine heart. In [11], Zheng *et al.* attempt to collect biomechanical energy from a biodegradable triboelectric nanogenerator. However, it is constrained by its susceptibility to humidity and friction. Apart from the aforementioned energy sources, another approach is to convert light that penetrates through human skin into electricity with a photovoltaic (PV) panel. Though human skin and subcutaneous tissues will block some light, there is a transparency window in the near-infrared (NIR) spectrum region where light passes the skin [12]. The work in [13] studies the properties of different silicon and GaAs PV cells within the NIR region, where a 850 nm microscope-compatible LED is used as the light source. Light in the NIR spectrum region is only a portion of the ambient light, thus S. Ayazian *et al.* attempt to use a 150 W halogen microscope illuminator to power a PV-driven implantable sensor [14]. A batteryless cardiac pacemaker with 3 monocrystalline solar cells is presented in [15], which demonstrates the real-life application by the in-vivo test in a pig. In [16], Bereuter *et al.* study the long-term operation of subcutaneous solar energy harvesting using an optical filter to substitute human skin. The average power harvested is about 67 μW with volunteers wearing the experimental device in their daily life.

The development of implantable biomedical sensors also requires appropriate wireless communication for data transmission [17], [18], which further increases power consumption. The work in [10] uses a flexible piezoelectric energy harvester to power a wirelessUSB NL development kit, and successfully switches on and off a light bulb placed 5 meters away. In this paper, a complete implantable sensor prototype with subcutaneous solar energy harvesting and wireless communication is proposed, as shown in Figure 1. The prototype incorporates a temperature sensor and a Bluetooth low energy (BLE) module in a transparent silicon housing. With the power from a flexible solar panel, it can measure the inner body temperature and send data to a mobile device, which can be a gateway for IoT-based healthcare monitoring. A long-term ex-vivo experiment (including two worst-case scenarios) of the implantable prototype is conducted to demonstrate the feasibility of a wireless implantable sensor design with subcutaneous energy harvesting.

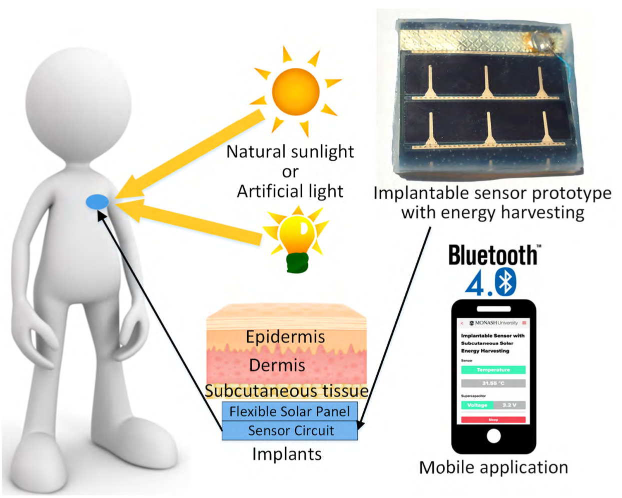

FIGURE 1. The proposed implantable sensor system prototype with subcutaneous solar energy harvesting.

The remainder of the paper is organized as follows: Section II presents the electrical properties of a flexible solar panel when covered by a 3 mm thick porcine skin flap under different ambient light conditions. In Section III, we compare the performance of the subcutaneous solar energy harvester on the different body parts (wrist, shoulder and neck). The implementation of the prototype's electrical components is described in Section IV. Section V demonstrates the experimental results of the prototype's long-term ex-vivo operation and two worst-case scenarios. The conclusion and future improvement of the work are discussed in the last section.

II. ELECTRICAL PROPERTIES OF A FLEXIBLE SOLAR PANEL UNDER SKIN

Solar energy harvesting has been adopted in many wearable biomedical sensor applications as an alternative to a battery [7], [19], [20]. However, the performance of the solar panel in an implantable sensor may be attenuated by the light absorption and scattering due to the skin and subcutaneous tissues. The research in [12] shows that skin has an optical transparency window (650-950 nm) in the NIR spectrum region where light can penetrate. E. Moon *et al.* propose a special PV cell with high efficiency in the NIR region for subcutaneous infrared energy harvesting, which uses a 850 nm LED as light source. In [14], a high-power (150 W) halogen microscope illuminator is utilized to power an implantable PV-driven sensor. In an initial work [21], we have studied the characteristics of a flexible solar panel under a porcine skin when illuminated by different ambient light. The solar panel used in this experiment, SP-37, is an off-the-shelf product from PowerFilm®. Several tests are conducted under different irradiance levels of sunlight and a 24 W bulb to evaluate its performance in real-life situations.

A. NATURAL SUNLIGHT

The electrical properties of the flexible solar panel under direct sunlight when covered by a 3 mm thick (1 mm skin and 2 mm fat) porcine flap are shown in Figure 2. Different irradiance levels are considered under different weather conditions, e.g. sunny day noon (1000 W/m^2), partly cloudy day (450 W/m^2), mostly cloudy day (150 W/m^2), and mostly

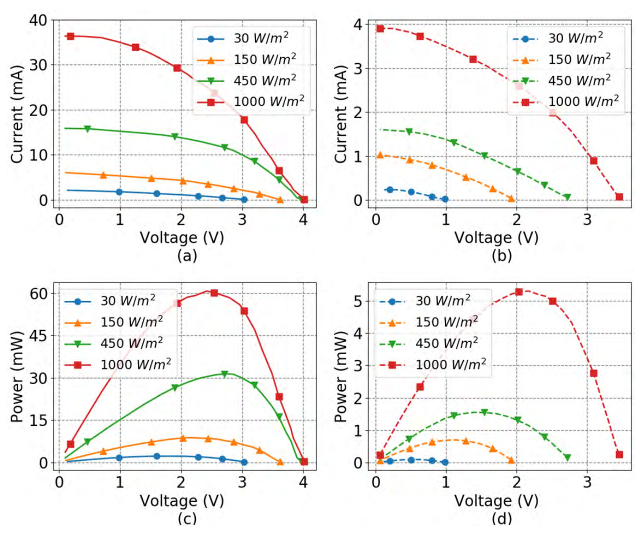

FIGURE 2. The measured characteristics of the flexible solar panel under natural sunlight: (a) I-V curve; (b) I-V curve (covered by porcine skin); (c) P-V curve; (d) P-V curve (covered by porcine skin).

cloudy day late-afternoon (30 W/m^2). The irradiance values are measured using a solar power meter, 1333R from TES®. As shown in Figure 2(d), the maximum power from the flexible solar panel covered by the porcine flap is around 5.5 mW under the best light situation (1000 W/m^2) and 90 μ under the worst light situation (30 W/m^2). According to the results in Figure 2 (c) and (d), the average power from the solar panel under the porcine flap is approximately 5% to 10% of that when exposed to direct sunlight.

B. ARTIFICIAL LIGHT

Figure 3 illustrates the performance of the flexible solar panel when illuminated by normal artificial light, a 24 W cool daylight fluorescent lamp bulb (1450 lm) from Philips® Tornado series. The lamp is placed at various distances to the solar panel for different irradiance conditions, e.g. 8 cm (40 W/m^2), 12cm (20 W/m^2), 16cm (10 W/m^2), and 22cm (4 W/m^2). The results in Figure 3(d) show that the maximum output power of the solar panel under the porcine flap varies from 100 μW to 1.4 mW at different distances. It is about 8% to 10% of that when directly illuminated by the lamp, which corresponds to results from the sunlight conditions.

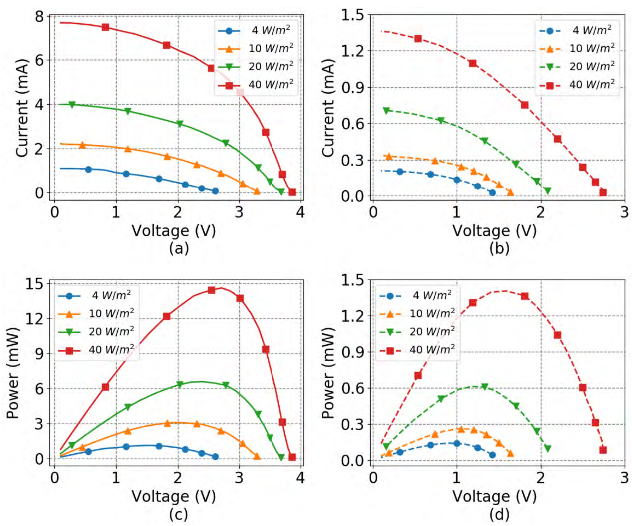

FIGURE 3. **The measured characteristics of the flexible solar panel under artificial light: (a) I-V curve; (b) I-V curve (covered by porcine skin); (c) P-V curve; (d) P-V curve (covered by porcine skin).**

In this section, the characteristics of a flexible solar panel covered by a 3 mm thick porcine flap are presented. The ex-vivo experimental results show that the solar panel can output tens of microWatts to a few milliWatts when covered under a porcine flap, depending on the light conditions. Although the power is about 5% to 10% of that when the solar panel is exposed to direct light, it is sufficient to power ultra low-power electronic circuits. A wireless implantable sensor prototype powered by the proposed subcutaneous energy harvester will be described in Section IV.

III. COMPARISON OF SOLAR ENERGY HARVESTING ON DIFFERENT BODY PARTS

The solar energy harvester may have varied performance on different body parts due to the exposure to light. To find an optimal position for solar energy harvesting, the flexible solar panel (covered by a porcine flap) is placed on different body parts (wrist, shoulder and neck), as shown in Figure 4. However, the light exposed to the harvester may be influenced by lots of other elements (buildings, trees, subject movement, etc.). The following procedures are taken to ensure the results are comparable:

- The experiments are conducted in an open area without other blocking.
- The experiments are conducted on a sunny day (no clouds) and a heavily cloudy day (no direct sunlight).
- The subject walks at a normal speed along a pre-defined track, as shown in Figure 5.

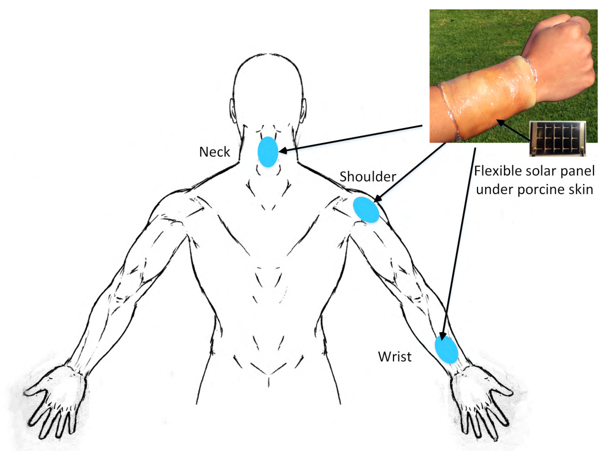

FIGURE 4. **The flexible solar panel covered by a porcine flap is placed on different body parts (wrist, shoulder and neck).**

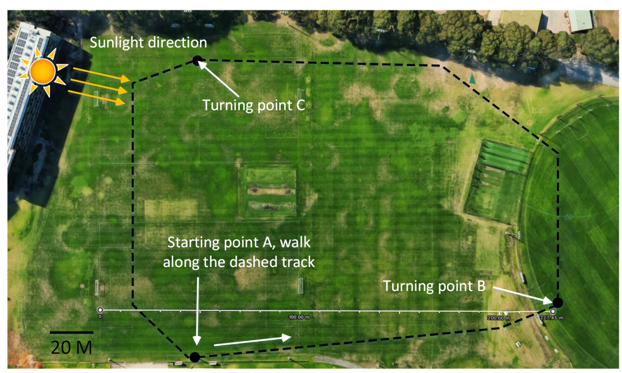

FIGURE 5. **The subject walks along a pre-defined track in an open area.**

The first experiment is taken on a sunny day noon (no clouds). The flexible solar panel covered by a 3 mm thick porcine flap is placed on a subject's wrist (right), shoulder (right) and neck, respectively. The solar panel is used to charge a 1 F supercapacitor through a power management circuit (will be discussed in Section IV). The subject walks at a normal speed along the track in Figure 5 for 2 cycles, and each cycle takes about 10 minutes. During the experiment the direct sunlight irradiance stays at a steady level, about 950 to 1000 W/m^2. The supercapacitor's voltage charged by the subcutaneous solar panel is illustrated in Figure 6. When the subject walks from starting point A to turning point B, the supercapacitor on the neck is in a fast charge period as the neck is exposed to the sunlight almost directly (with a small angle). From point B to point C the neck is in an opposition direction to sunlight, thus the supercapacitor on the neck is in a slow charge period. For the supercapacitor on the right wrist or right shoulder, it is charged slowly from point A to point C because of no direct exposure to sunlight. From point C to point A the neck supercapacitor is charged faster than from B to C but slower than from A to B, as the neck is exposed to sunlight with a large angle. The voltage of the supercapacitor on the right wrist or right shoulder increases quickly from point C to point A due to the exposure to sunlight. Because the wrist is lower and swings more than the shoulder, the supercapacitor on the wrist is charged slower than that on the shoulder by the flexible solar panel under a porcine flap. For the second cycle in Figure 6, the voltage curves of the supercapactor charged by the subcutaneous solar panel on different body parts repeat a similar pattern, except the supercapacitor on the neck reaches an overcharge protection voltage.

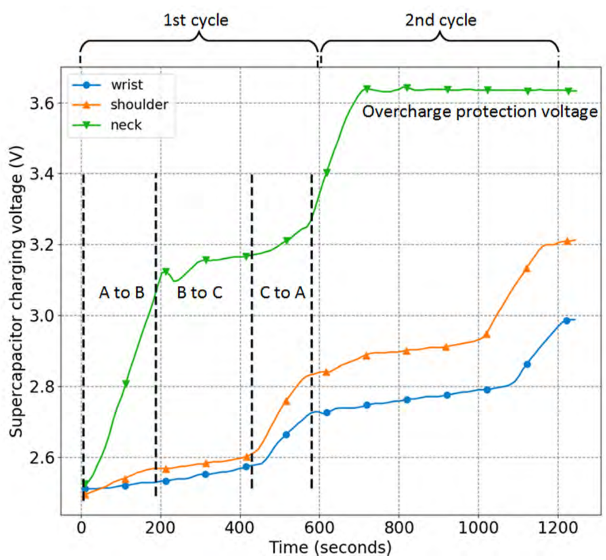

FIGURE 6. **The voltage of a 1 F supercapacitor charged by a flexible solar panel placed on different body parts on a sunny day.**

Figure 7 shows the experimental results on a heavily cloudy day (the sun is totally blocked by cloud). The irradiance level during the experiment varies from 100 to 200 W/m^2 which is caused by cloud movement. In this experiment there is no distinctive fast or slow charge period of the supercapacitor because there is no direct exposure to sunlight. However, the supercapacitor on the upper body (shoulder and neck) is charged faster than that on the wrist. The explanation

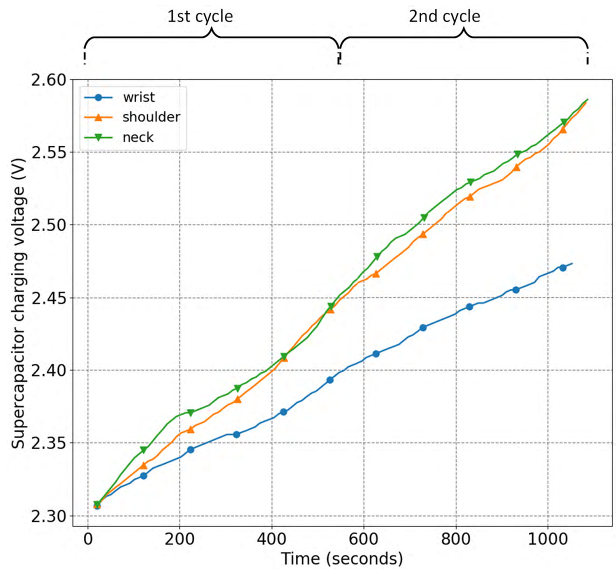

FIGURE 7. **The voltage of a 1 F supercapacitor charged by a flexible solar panel placed on different body parts on a heavily cloudy day.**

is that wrist is less exposed to light due to the shadow of the body and wrist movement. The results in Figure 6 and 7 show that solar energy harvester on the neck outperforms those on the other body parts. However, the power harvested may be affected by many other shadows from the ambient in a real-life situation. Considering the body structure and clothing, the upper body area between the neck and shoulder may be an optimal position for subcutaneous solar energy harvesting.

IV. IMPLEMENTATION OF THE IMPLANTABLE SENSOR PROTOTYPE WITH ENERGY HARVESTING

In this section, an implantable sensor prototype powered by the subcutaneous solar energy harvester is presented. The prototype consists of a power management circuit, a temperature sensor and a wireless communication module. A mobile application for sensor data visualization will also be described. As the power from the subcutaneous solar panel is in the range of microWatts to a few milliWatts (maximum), the power consumption of the prototype needs to be ultra low for long-term operation.

A. POWER MANAGEMENT CIRCUIT

The maximum power point tracking (MPPT) circuit is significant to solar energy harvesting, as the power from a solar panel varies a lot depending on the irradiance level and ambient temperature [22]. In this work, a power management IC, BQ25505 from Texas Instrument®, is exploited to maximize the power from the solar panel. BQ25505 has an embedded MPPT algorithm based on the fraction open circuit voltage (FOCV) method. The FOCV algorithm proposes the voltage of a solar panel at the maximum power point is proportional to its open circuit voltage [23]. As shown in Figure 2(d) and 3(d), the maximum power point voltage of the flexible solar panel covered under a porcine flap is between 60% to 70% of its open circuit voltage. Therefore we set a reference of 66.7% to BQ25505, which samples and updates the maximum power point every 16 seconds.

B. TEMPERATURE SENSOR

Temperature is a vital signal of the human body, and an implantable temperature sensor has potential medical applications such as inner body localized temperature monitoring and heating detection of other implants [24]. A high accuracy (0.1°C from 37°C to 39°C) and low-power (600 μA at 2.7 V to 3.3 V) temperature IC, the MAX30205 from Maxim®, is implemented in this prototype. The MAX30205 is used in its one-shot mode, which sets the sensor to sleep (3.5 μA) most of the time and wakes it up periodically for a temperature measurement (600 μA) in a few milli seconds.

C. WIRELESS COMMUNICATION

Wireless transmission is a critical part in an implantable sensor system, which enables the communication between inner body and outside. However, its relatively high-power consumption raises new challenge to the power system of an implant. The proposed prototype incorporates a professional grade BLE module to transmit the implanted sensor data to a mobile device (a smartphone or tablet). The BLE module, RFD77101, has an on-chip antenna and a built-in microcontroller (ARM Cortex M0) for data processing before transmission. The peak transmission current of RFD77101 is about 8 mA, while its sleep current (with clock running) is less than 4 μA. In this work, a web-based application on the Evothings® platform is developed to display sensor data on a mobile device.

All the electronic components are implemented on a small flexible PCB (33 mm × 27 mm), as shown in Figure 8(a). The flexible PCB is covered by the aforementioned solar panel, which is folded in half to reduce the size. The entire device is embedded into a transparent silicone rubber housing, which is created using Ecoflex 00-10 from Smooth-On®. The cured rubber housing is soft, but strong and stretchy, as shown in Figure 8(b). Figure 8(c) describes the application for the display of the implantable sensor data, which can be run on a smartphone or tablet with Bluetooth 4.0 technology.

D. POWER CONSUMPTION

An implantable sensor needs to be ultra low-power for long-term operation without intervention. The proposed system works at 2.7 V, the minimum voltage of the temperature sensor. Figure 9 demonstrates the current of the entire prototype at different operation mode. Although the peak transmission current of the BLE module is 8 mA, the average working current is between 400 to 500 μA for 5 seconds. This is because data is transmitted once when acknowledged immediately, or maximum three times when no acknowledgement received. The sleep current with clock running is around 7 μA. By calculation, the average power of proposed implantable sensor prototype is 130μW (average 48 μA at 2.7 V) for a 1 minute cycle (sleep for 55 seconds), and 30 μW (average 11 μA at 2.7 V) for a 10 minutes cycle (sleep for 595 seconds).

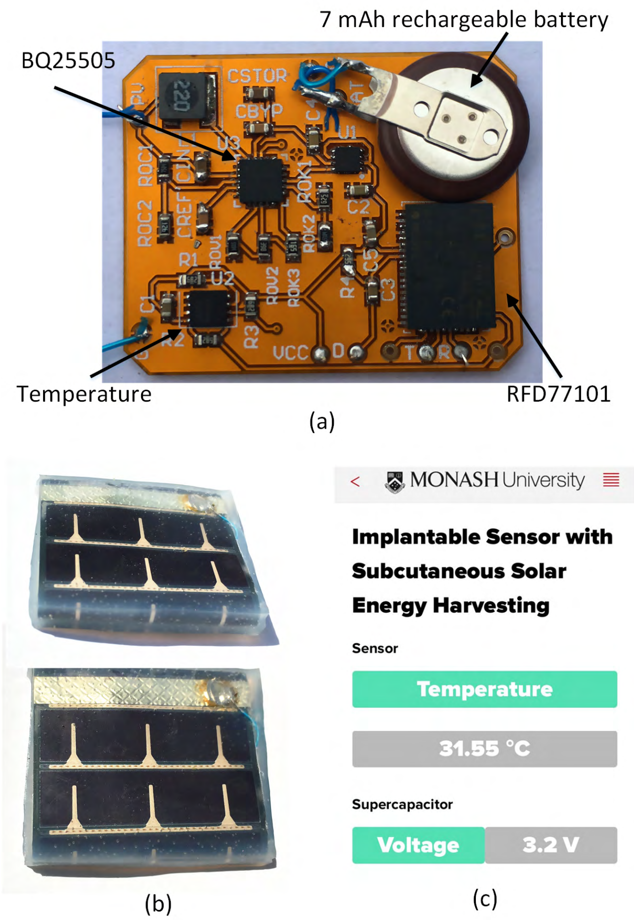

FIGURE 8. The proposed implantable sensor prototype: (a) A flexible PCB for electronic components (33 mm × 27 mm); (b) The entire prototype in a stretchy transparent silicone housing (38 mm × 32 mm × 4 mm); (c) An application for sensor data visualization.

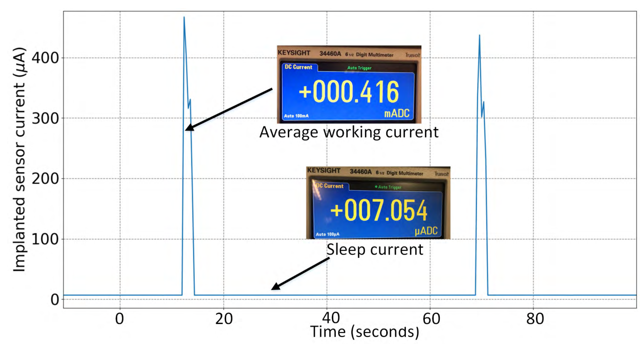

FIGURE 9. The current of the proposed implantable sensor prototype in a 1 minute operation cycle.

V. LONG-TERM OPERATION EXPERIMENTS

In section II, the electrical properties of the flexible solar panel under different light conditions are presented. According to the results of the ex-vivo experiments, the output power from the solar panel (under a 3 mm thick porcine flap) varies between 60 μW to 5.5 mW depending on the light source.

In the proposed implantable prototype the flexible solar panel is folded, thus the harvesting power will be approximately half of the results in Section II. It is still sufficient for the proposed low-power sensor prototype, especially under good light conditions (on a sunny day or close to a lamp).

Considering the power consumption and data measurement requirements, the proposed implantable sensor prototype is set to a 10 minutes operation cycle. It sleeps (7 μA) for 595 seconds and wakes up (average 400 to 500 μA) for about 5 seconds to initialize BLE, connect to an end device, measure temperature, send data, and receive acknowledgement. During the wake-up 5 seconds, most of the time it is also set to a low-power mode between different tasks to minimize power consumption. The average power of the 10 minutes operation cycle is about 30 μW (average 11 μA at 2.7 V). According to Figure 2(d) and 3(d), the maximum harvesting power of the solar panel under a porcine flap is about 5 mW and 1.4 mW when exposed to direct sunlight or close to a 24 W lamp (8 cm away), respectively. As for the proposed subcutaneous energy harvester with a folded solar panel, the power is about half of that from a full solar panel, which is 2.75 mW and 0.7 mW. This means the energy harvested in 1 or 2 hours under good light condition (direct sunlight or close to a lamp light) can provide enough energy for the implantable sensor prototype to work for an entire day. An ex-vivo experiment is conducted to evaluate the long-term performance of the proposed prototype, as shown in Figure 10. To meet potential worst-case scenarios (will be discussed in next paragraph), a 7 mAh rechargeable battery, VL1220 from Panasonic®, is selected for energy storage. The battery is small in size (∅12 mm × 2 mm) thus can be embedded in the prototype housing in Figure 8(b). The ex-vivo experiment is carried out with the proposed sensor prototype covered under a 3 mm thick porcine flap. Every day it is illuminated by a 24 W cool daylight fluorescent lamp for 1 hour, after which it is placed in a complete dark box for the rest of the day. As shown in Figure 10, the proposed prototype successfully works for 12 days under the experimental condition with the battery voltage drops less than 0.2 V. Given better light conditions, such as exposure to direct sunlight or longer time to the lamp, the battery can be expected to stay fully charged.

Considering some potential real-life issues, two worst-case scenarios are simulated with experiments:

(1) No exposure to light

A 7 mAh rechargeable battery is selected for energy storage when there is no light exposure for a long period. To make things worse, the implantable sensor prototype is set to a 1 minute operation cycle for relatively high-power consumption 130 μW (average 48 μA at 2.7 V). In this extreme case, the proposed prototype can work for 100 hours only powered by the battery, as shown in Figure 11. It is less than the theoretical 146 hours (7 mAh / 48 μA), as there is power loss and battery lifetime is shortened by high-power consumption.

(2) Complete battery depletion

Another worst-case is when the implanted battery is completely discharged. Experiment shows the battery can be charged from depletion by the subcutaneous energy harvester, which is covered by a 3 mm thick porcine flap. According to Figure 12, it takes about 24 hours to charge the depleted battery to a high voltage status when illuminated by a 24 W lamp (average current is about 200 μA). This demonstrates

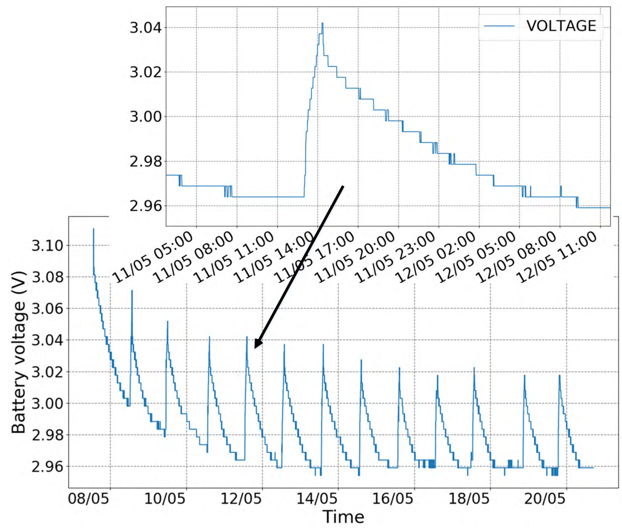

FIGURE 10. The battery voltage in the long-term experiment, during which the prototype is illuminated by a 24 W lamp for 1 hour every day.

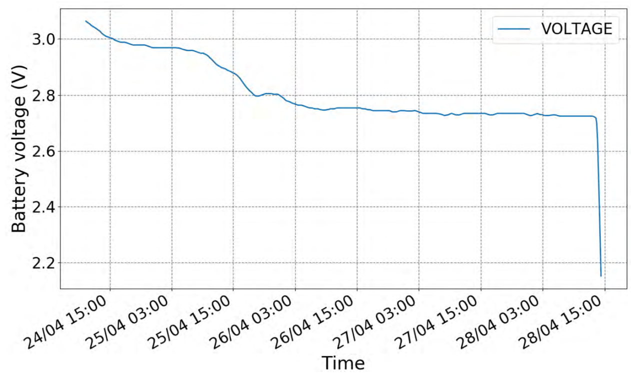

FIGURE 11. The sensor prototype can work for 100 hours when powered only by a 7 mAh battery.

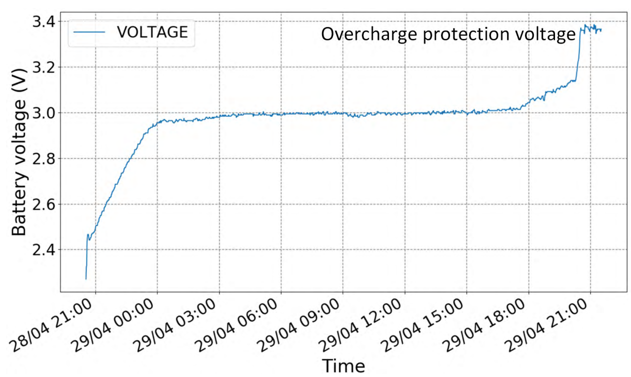

FIGURE 12. Charging a completely depleted battery embedded in the proposed implantable prototype.

TABLE 1. Comparisons of implantable medical systems with subcutaneous energy harvesting.

	[10]	[14]	[15]	[13]	This work
Energy source	Heartbeat	Halogen lamp	Sunlight	Infrared light	Sunlight & fluorescent lamp
Energy harvester	Piezoelectric	Photovoltaic cell	Solar panel	Photovoltaic cell	Flexible solar panel
Energy harvester area (mm)	20×30	2.5×2.5	22×7 (3 pieces)	1.22×1	37×32 (folded)
Power [(a)]	OCV: 17.8 V SCC: 1.74 μA [(b)]	19.2 nW/mm^2 [(c)]	19.63 μW/mm^2 [(d)]	100 nW/mm^2 [(e)]	2.32 μW/mm^2 [(f)]
Application	——	Neuromorphic signal	Pacemaker	——	Temperature
Wireless communication	WirelessUSB NL Development Kit	——	——	——	BLE
Total size (mm)	——	$4 \times 4 \times 0.5$	$30 \times 35 \times 6$	——	$38 \times 32 \times 4$

[a] Power from different energy harvesters varies a lot due to experimental conditions. Here are some reference values.
[b] OCV is abbreviation for open-circuit voltage, and SCC is abbreviation for short-circuit current.
[c] Measured under 3 mm thick bovine muscle and chicken skin, exposed to a 150 W halogen illuminator.
[d] Measured under 4.8 mm thick porcine skin, exposed to full sunlight.
[e] Measured under 3 mm thick porcine skin, exposed to 1.08 μW/mm^2 infrared light (850 nm).
[f] Measured under 3 mm thick porcine skin. Maximum power is 2.32 μW/mm^2 when exposed to full sunlight, and 0.59 μW/mm^2 when illuminated by a 24 W fluorescent lamp.

that the proposed sensor prototype can be restarted even when battery is depleted.

In Table 1, the comparison between different implantable biomedical systems with energy harvesting is presented.

VI. CONCLUSION

This paper proposes a subcutaneous solar energy harvester for implantable biomedical devices. The electrical properties of a flexible solar panel under a porcine flap are studied under sunlight and artificial light sources. The output power of the subcutaneous solar panel varies from tens of microWatts to a few milliWatts depending on irradiance levels. An optimal position for the subcutaneous energy harvester is found to be between the neck and shoulder, which is demonstrated by ex-vivo experiments. To evaluate the real-life application of the harvester, a wireless implantable sensor prototype is presented. The prototype incorporates a power management circuit, a temperature sensor, a BLE module and a 7 mAH rechargeable battery, which are all embedded in a transparent silicone housing. The sensor system is set to a 10 minutes operation cycle with power of 30 μW, which can be self-powered by the subcutaneous solar energy harvester. The long-term operation, including two worst-case scenarios (no exposure to light and battery depletion), are demonstrated by ex-vivo experimental results. In the future, the work can be improved by dedicated solar panels that are more suitable for subcutaneous light conditions. The potential flexible supercapacitor can be used to replace the battery, which can further reduce the volume of the implantable prototype.

REFERENCES

[1] U. E. Bauer, P. A. Briss, R. A. Goodman, and B. A. Bowman, "Prevention of chronic disease in the 21st century: Elimination of the leading preventable causes of premature death and disability in the USA," *Lancet*, vol. 384, no. 9937, pp. 45–52, 2014.
[2] A. Kiourti and K. S. Nikita, "A review of in-body biotelemetry devices: Implantables, ingestibles, and injectables," *IEEE Trans. Biomed. Eng.*, vol. 64, no. 7, pp. 1422–1430, Jul. 2017.
[3] A. Haeberlin *et al.*, "Successful pacing using a batteryless sunlight-powered pacemaker," *Europace*, vol. 16, no. 10, pp. 1534–1539, 2014.
[4] S. Vaddiraju, M. Kastellorizios, A. Legassey, D. Burgess, F. Jain, and F. Papadimitrakopoulos, "Needle-implantable, wireless biosensor for continuous glucose monitoring," in *Proc. 12th Int. Conf. Wearable Implant. Body Sensor Netw. (BSN)*, Cambridge, MA, USA, Jun. 2015, pp. 1–5.
[5] R. Muller *et al.*, "A minimally invasive 64-channel wireless μECoG implant," *IEEE J. Solid-State Circuits*, vol. 50, no. 1, pp. 344–359, Jan. 2015.
[6] M. A. Hannan, S. Mutashar, S. A. Samad, and A. Hussain, "Energy harvesting for the implantable biomedical devices: Issues and challenges," *Biomed. Eng. Online*, vol. 13, no. 1, p. 79, 2014.
[7] T. Wu, F. Wu, J.-M. Redouté, and M. R. Yuce, "An autonomous wireless body area network implementation towards IoT connected healthcare applications," *IEEE Access*, vol. 5, pp. 11413–11422, 2017.
[8] A. B. Amar, A. B. Kouki, and H. Cao, "Power approaches for implantable medical devices," *Sensors*, vol. 15, no. 11, pp. 28889–28914, 2015.
[9] S. Stoecklin, A. Yousaf, T. Volk, and L. Reindl, "Efficient wireless powering of biomedical sensor systems for multichannel brain implants," *IEEE Trans. Instrum. Meas.*, vol. 65, no. 4, pp. 754–764, Apr. 2016.
[10] D. H. Kim *et al.*, "*In vivo* self-powered wireless transmission using biocompatible flexible energy harvesters," *Adv. Funct. Mater.*, vol. 27, no. 25, p. 1700341, 2017.
[11] Q. Zheng *et al.*, "Biodegradable triboelectric nanogenerator as a life-time designed implantable power source," *Sci. Adv.*, vol. 2, no. 3, p. e1501478, 2016.
[12] A. N. Bashkatov, E. A. Genina, V. I. Kochubey, and V. V. Tuchin, "Optical properties of human skin, subcutaneous and mucous tissues in the wavelength range from 400 to 2000 nm," *J. Phys. D, Appl. Phys.*, vol. 38, no. 15, p. 2543, 2005.

[13] E. Moon, D. Blaauw, and J. D. Phillips, "Subcutaneous photovoltaic infrared energy harvesting for bio-implantable devices," *IEEE Trans. Electron Devices*, vol. 64, no. 5, pp. 2432–2437, May 2017.
[14] S. Ayazian, V. A. Akhavan, E. Soenen, and A. Hassibi, "A photovoltaic-driven and energy-autonomous CMOS implantable sensor," *IEEE Trans. Biomed. Circuits Syst.*, vol. 6, no. 4, pp. 336–343, Aug. 2012.
[15] A. Haeberlin *et al.*, "The first batteryless, solar-powered cardiac pacemaker," *Heart Rhythm*, vol. 12, no. 6, pp. 1317–1323, 2015.
[16] L. Bereuter *et al.*, "Energy harvesting by subcutaneous solar cells: A long-term study on achievable energy output," *Ann. Biomed. Eng.*, vol. 45, no. 5, pp. 1172–1180, 2017.
[17] A. F. Demir *et al.*, "*In vivo* communications: Steps toward the next generation of implantable devices," *IEEE Veh. Technol. Mag.*, vol. 11, no. 2, pp. 32–42, Jun. 2016.
[18] Q. H. Abbasi, A. A. Nasir, K. Yang, K. A. Qaraqe, and A. Alomainy, "Cooperative *in-vivo* nano-network communication at terahertz frequencies," *IEEE Access*, vol. 5, pp. 8642–8647, 2017.
[19] W. Y. Toh, Y. K. Tan, W. S. Koh, and L. Siek, "Autonomous wearable sensor nodes with flexible energy harvesting," *IEEE Sensors J.*, vol. 14, no. 7, pp. 2299–2306, Jul. 2014.
[20] A. Dionisi, D. Marioli, E. Sardini, and M. Serpelloni, "Autonomous wearable system for vital signs measurement with energy-harvesting module," *IEEE Trans. Instrum. Meas.*, vol. 65, no. 6, pp. 1423–1434, Jun. 2016.
[21] T. Wu, J.-M. Redoute, and M. R. Yuce, "Subcutaneous solar energy harvesting for self-powered wireless implantable sensor systems," in *Proc. 40th Annu. Int. Eng. Med. Biol. Conf.*, Honolulu, HI, USA, Jul. 2018.
[22] V. Salas, E. Olias, A. Barrado, and A. Lazaro, "Review of the maximum power point tracking algorithms for stand-alone photovoltaic systems," *Sol. Energy Mater. Sol. Cells*, vol. 90, no. 11, pp. 1555–1578, 2006.
[23] J. Ahmad, "A fractional open circuit voltage based maximum power point tracker for photovoltaic arrays," in *Proc. 2nd Int. Conf. Softw. Technol. Eng. (ICSTE)*, San Juan, PR, USA, vol. 1, Oct. 2010, pp. V1-247–V1-250.
[24] Y.-J. Hung *et al.*, "High-voltage backside-illuminated CMOS photovoltaic module for powering implantable temperature sensors," *IEEE J. Photovolt.*, vol. 8, no. 1, pp. 342–347, Jan. 2018.

TAIYANG WU (S'16) received the B.E. degree from Southeast University, Nanjing, China, in 2014. He is currently pursuing the Ph.D. degree in electrical and computer systems engineering with Monash University. His main areas of research interest are energy harvesting, biomedical sensor network, and IoT connected health monitoring applications.

JEAN-MICHEL REDOUTÉ (M'09–SM'12) received the M.S. degree in electronics from the University College of Antwerp, Belgium, in 1998, the M.Eng. degree in electrical engineering from the University of Brussels, Belgium, in 2001, and the Ph.D. degree in design of EMI resisting analog integrated circuits in 2009. In 2001, he started working at Alcatel Bell, Antwerp, where he was involved in the design of analog microelectronic circuits for telecommunications systems. In 2005, he joined ESAT-MICAS laboratories, University of Leuven, as a Ph.D. Research Assistant. In 2009, he started working at the Berkeley Wireless Research Center, University of California at Berkeley, Berkeley, as a Post-Doctoral Scholar. In 2010, he joined Monash University as a Senior Lecturer. His research interests include mixed-signal integrated circuit design, electromagnetic compatibility, biomedical (integrated and non-integrated) circuit design, and radio-frequency integrated circuit design.

MEHMET RASIT YUCE (S'01–M'05–SM'10) received the M.S. degree in electrical and computer engineering from the University of Florida, Gainesville, FL, USA, in 2001, and the Ph.D. degree in electrical and computer engineering from North Carolina State University, Raleigh, NC, USA, in 2004. He was a Post-Doctoral Researcher with the Electrical Engineering Department, University of California at Santa Cruz, in 2005. He was an Academic Member with the School of Electrical Engineering and Computer Science, University of Newcastle, Callaghan, NSW, Australia, until 2011. In 2011, he joined Monash University, Australia, where he is currently an Associate Professor with the Department of Electrical and Computer Systems Engineering.

He has authored the books *Wireless Body Area Networks* (2011) and *Ultra-Wideband and 60 GHz Communications for Biomedical Applications* (2013). His research interests include wearable devices, Internet-of-Things for healthcare, wireless implantable telemetry, wireless body area network, bio-sensors, integrated circuit technology dealing with digital, analog and radio frequency circuit designs for wireless, biomedical, and RF applications. He has published over 150 technical articles in the above areas. He received the NASA Group Achievement Award in 2007 for developing an SOI transceiver, the Best Journal Paper Award in 2014 from the IEEE Microwave Theory and Techniques Society, and the Research Excellence Award from the Faculty of Engineering and Built Environment, University of Newcastle, in 2010. He is a Topical Editor for the IEEE Sensors Journal and a Guest Editor for the IEEE Journal of Biomedical and Health Informatics in 2015.